Tourmalines of the povondraite – (oxy)dravite series from the cap rock of meta-evaporite in Alto Chapare, Cochabamba, Bolivia

Turmalíny řady povondrait – (oxy)dravit ze sádrovcového klobouku metaevaporitu v Alto Chapare, provincie Cochabamba, Bolívie

(8 text-figs, 4 tabs)

VLADIMÍR ŽÁČEK[1] – JIŘÍ FRÝDA[1] – ALFRED PETROV[2] – JAROSLAV HYRŠL[3]

[1] *Czech Geological Survey, P. O. Box 85, Klárov 3, 118 21, Praha 1, Czech Republic*
[2] *P. O. BOX 1728, Cochabamba, Bolivia*
[3] *Heverova 222, 280 00, Kolín 4, Czech Republic*

An almost continuous series of Al-deficient ferrian tourmalines, corresponding mainly to povondraite – "oxy-dravite" – dravite solid solutions, was found at the type locality of povondraite (Alto Chapare, Cochabamba Department, Bolivia). These tourmalines form a component of crystalline crusts overgrowing silicate "xenoliths" or loose crystals enclosed in the meta-evaporite cap rock. Tourmaline crystals have highly variable morphology, correlated with chemical composition from acicular through prismatic to stubby. Some crystals are discontinuously zoned with Al-enriched cores. Tourmalines are typically sodic with very low Ca and low X-site vacancy. On the other hand, Fe-rich, Al-poor tourmalines have elevated K content (up to 0.6 *apfu*) in a trend toward a new tourmaline species. All tourmalines are magnesian (Mg = 1.32–2.67 *apfu*) and display extreme compositional range. The most prominent substitution of Fe^{3+} (0.31–7.58 *apfu*) for Al (0.03–5.81 *apfu*) is represented by the exchange vector $Fe^{3+}(Al)_{-1}$. Fe-rich members form a transitions between povondraite [$NaFe_3^{3+}(Mg_2Fe_4^{3+})Si_6O_{18}(BO_3)_3(OH)_3O$] and hypothetical tourmaline [$NaFe_3^{3+}(Mg_1Fe_5^{3+})Si_6O_{18}(BO_3)_3((OH)_2O)O$]. In accordance with this substitution mechanism, the OH_{calc} ranging from 1.78–3.52 *pfu* is positively correlated with Mg and inversely proportional to the sum of R^{3+} (= Al + Fe^{3+}). Incorporation of Ti^{4+} in tourmaline solid solution is coupled with a decrease of OH and an increase of O. The highly variable Ti (0.0–0.56 *apfu*) negatively correlates with the sum of R^{3+}. However, there also is an excellent negative correlation (R = 0.99) among R^{3+} and Mg+Ti. This is consistent with exchange vectors $R^{3+}O(Mg\ OH)_{-1}$ and $TiOR^{3+}_{-1}(OH)_{-1}$. Such substitutions suggest a new possible Ti-bearing tourmaline $Na(TiR^{3+}_2)(Mg_2R^{3+}_4)Si_6O_{18}(BO_3)_3((OH)_2O)O$. The povondraite – (oxy)dravite solid solutions are known in meta-evaporite tourmalines but only the tourmalines from the Bolivian Alto Chapare attained such an extensive compositional range.

Key words: tourmaline, povondraite, "oxy-dravite", dravite, ferrian, chemical composition, meta-evaporite

Introduction

Tourmalines occur with many associated minerals in a highly unusual rock called the Locotal Breccia, a brecciated metamorphosed evaporite cap rock (Petrov *et al.* 1997, Žáček *et al.* 1998). The Locotal Breccia outcrops sporadically within a roughly 50 km² area of deeply dissected rain-forest topography in the Alto Chapare region, Cochabamba Department, Bolivia, in steep eastern foothills of the Andes at an altitude between 400 to 2000 metres (Fig. 1). The Locotal Breccia is composed mainly of dolomite, magnesite, gypsum, anhydrite, K-feldspar, smectites and minor danburite, boracite, hematite, pyrite and rutile. It encloses angular cm- to dm- sized clasts or "xenoliths" of various silicate-rich rocks which mostly represent highly alkaline rocks, probably volcanics. Tourmalines form crystal crusts overgrowing the clasts (Fig. 2) or they occur as loose crystals enclosed directly in the cap rock minerals. Besides tourmaline, the clasts are overgrown by crystals of microcline, less frequently of magnesioriebeckite, aegirine, magnesite, ankerite, hematite, and pyrite. The samples occurring as loose chips on the surface in tropical rainforest represent poorly soluble metaevaporite fraction accumulated in the cap rock (Franz *et al.* 1979, Petrov 1994, Žáček *et al.* 1998).

Fig. 1. Location of the povondraite locality in Alto Chapare (solid square).

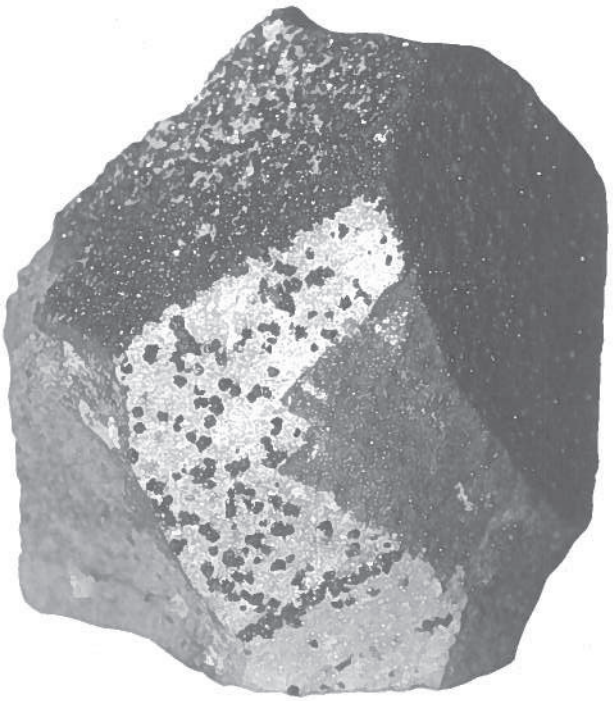

Fig. 2. Angular clast (10x8x7 cm) overgrown by tourmaline crystals (# 1).

Povondraite, a new member of the tourmaline group, has an interesting history. The first specimen was collected in the San Francisco mine by Dr. W. Wetzenstein during his study of magnesite deposits in Chapare (Franz *et al.* 1979). The specimen was studied by Walenta – Dunn (1977) and they described it as a new tourmaline ferridravite. A new crystallographic study of Grice *et al.* (1993) showed that it is in fact a Fe^{3+} analog of buergerite, with the composition of $Na\ Fe_3^{3+}Fe_6^{3+}\ Si_6O_{18}\ (BO_3)_3\ (O,OH)_4$. Therefore a new name "povondraite" was proposed after the Czech mineralogist and well-known tourmaline specialist Dr. P. Povondra. New study of Hawthorne – Henry (1999) shows that Mg participates in the formula and in accordance with the requirement of electroneutrality, the ideal end-member formula of ordered povondraite may be written as:

$Na\ Fe_3^{3+}(Mg_2Fe_4^{3+})Si_6O_{18}\ (BO_3)_3\ (OH)_3\ O.$

This formula is in agreement with our new compositional data. The present paper contributes compositional data on a unique tourmaline assemblage from an ancient meta-evaporite cap rock at the type locality of povondraite in Alto Chapare, Cochabamba Department, Bolivia. Substitution mechanism in the povondraite – (oxy)dravite series is described, as well as the roles of K and Ti.

Samples and methods

The samples examinated were collected at the type locality of povondraite (Alto Chapare, Cochabamba Department, Bolivia) by A. P. and J. H. mainly during the last decade. Textural relations of tourmalines and associated minerals and their optical properties were studied in thin sections (samples B–1 – B–4, for details see Žáček *et al.* 1998) and in polished sections. Because tourmaline specimens are found as isolated clusters grown in the cap rock breccia or as loose specimen in eluvia, each of them represents a unique specimen more or less differing from another (see Appendix). This is reflected in highly variable chemistry: among the samples studied, there are hardly two samples with the same chemical composition. The most common clasts are fine-grained to medium-grained, composed of microcline and minor phlogopite; bluish clasts contain in addition magnesioriebeckite. Tourmaline intensively replaces some clasts, with the abundance of tourmaline increasing toward the clast rim; even cm-thick marginal zones of such clasts can be nearly completely replaced by massive tourmaline. Crystal crusts covering light-colored sandstone-like clasts are mostly sharply bound. Two samples with tourmaline enclosed as individual crystals in dolomite and danburite were also studied. Tourmaline crystals display variable morphology, which correlates with their chemical composition, from acicular (dravitic, Fe-poor) via prismatic (aluminous – ferrian) to stubby (aluminous povondraite to povondraite) forms (see Appendix).

Chemical compositions were analysed by EMPA (Czech Geological Survey, supervised by I. Vavřín), using an electron microprobe and CamScan 4–90DV equipped with Link-eXL-Oxford Instruments (EDX). The analyses using the energy-dispersive system Link-eXL were preferred for the following reasons. The X-ray signals of all analyzed elements are counted at the same time and so analytical results are affected by the same drift error. Thus, the possible drift error does not affect the ratio of analyzed elements. Also an optimum beam current for EDS is several times lower than that used for wavelength-dispersive methods; consequently, lower analytical errors in Na and K values were found because of reduced volatilization of these elements. Accelerating voltage of 15 kV, beam current 3 nA, and counting time 80 seconds were used. Natural minerals were used as standards for Si (quartz), Al (corundum), Ca (wollastonite), Ti (rutile), K (adularia; orthoclase – MAC registered standard No. 2726), Na (albite – MAC registered standard No. 2726), and synthetic olivines for Mg, Fe, and Mn (forsterite, fayalite, and tephroite). Measured concentrations were corrected by the ZAF model, assuming the presence of boron and absence of fluorine. Tourmaline formulae were normalized to 15 $T+Z+Y$ cations (exclusive Na, K and Ca in X, i. e. assuming no vacancies in tetrahedral and octahedral sites and insignificant Li contents (see Henry – Dutrow 1996). Based on substitution trends in tourmaline and a highly oxidized parent assemblage (see below), all Fe is assumed to be trivalent. Consequently, calculation of OH is based on charge balance constraints. We have not attempted to assign the cations to the specific Z and Y sites in any ordered fashion, as the distribution of Al, Fe and Mg into the two sites is impossible without a single-crystal structure refinement (Grice *et al.* 1993). The analytical results are summarized in Figures 4–8 and Tables 1–4.

Substitution mechanism

Alto Chapare tourmaline crystals typically show a discontinuous two-stage growth with more aluminous cores (Fig. 3). Tourmalines also exhibit extreme compositional variations involving dominantly Fe and Al but also Mg, Ti, Na, and K. The tourmalines belong to alkali group of tourmalines, having low Ca content and negligible to zero *X-site vacancy*. Also the Li, F, Mn, Cr, and V are very low (Walenta – Dunn 1974, Grice *et al.* 1993, Žáček *et al.* 1998). As shown on Fig. 4a, the compositional variability is principally controlled by solid solution among three end-member compositions: povondraite (ordered), "oxy-dravite" and dravite (with formulae of ordered povondraite and hypothetical tourmaline "oxy-dravite" recently proposed by Hawthorne – Henry 1999):

povondraite: $NaFe_3^{3+}(Mg_2Fe_4^{3+})Si_6O_{18}(BO_3)_3(OH)_3O$
"oxy-dravite": $Na(MgAl_2)(MgAl_5)Si_6O_{18}(BO_3)_3(OH)_3O$
dravite: $NaMg_3Al_6Si_6O_{18}(BO_3)_3(OH)_3(OH)$

Assuming stoichiometric B=3, there are two unknown quantities in our tourmalines: OH and Fe^{3+}. As a first approximation we consider all iron to be trivalent. This assumption is supported by the following facts: **1.** The tourmaline assemblage includes ferric minerals as aegirine, hematite and magnesioriebeckite; **2.** The highly variable Al is dominantly substituted by Fe, ($FeAl_{-1}$ exchange vector). A linear least-squares fit of the Al (total) plotted versus Fe (total) yielded a regression of Fe = –1.12 * Al + 7.21 [R=0.977], (Fig. 5); **3.** Cap rock and metaevaporite tourmalines reported in the literature are principally all ferrian (Henry *et al.* 1999).

The assumption that all iron is trivalent permits quantitative estimates of OH using charge-balance constraints (Tables 2–4). The calculated OH is highly variable in the range from 1.78 to 3.52 OH *pfu*. Mg is variable over a comparable range, and it varies from 1.32 to 2.67 *pfu*, exhibiting negative correlation with $\sum R^{3+}$ (= $Al^{3+} + Fe^{3+}$), Fig. 6a. This correlation implies the deprotonation substitution:

$Mg^{2+} + (OH)^{1-} = R^{3+} + O^{2-}$ (*i. e.*, the $R^{3+}O(Mg\ OH)_{-1}$ exchange vector) elegantly documented by Henry *et al.* (1999) for authigenic cap rock tourmalines from Challenger Knox. In fact, this substitution (assuming Fe-free end-members) represents an exchange vector between dravite (Mg = 3 *apfu*, Mg/Al = 0.5, OH = 4) and "oxy-dravite" (Mg = 2 *apfu*, Mg/Al = 0.286, OH = 3). A linear least-square fit of Mg vs. OH (Fig. 6b) yields a regression OH = 1.01 * Mg + 0.78 [R=0.780]; similarly the fit of R^{3+} vs. Mg yielded R^{3+} = –0.80 * Mg + 7.42 [R=0.781]. As apparent from Fig. 6a, b and from the above equations, the correlation is not as excellent as that of Henry *et al.* (1999). This is because the Alto Chapare tourmalines also contain highly variable but mostly significant amounts of Ti, varying from 0.0 to 0.56 *apfu* (equal a maximum of 4 wt. % TiO_2). The highest Ti concentrations recorded here match the uppermost concentrations very rarely attained in tourmaline (see Henry – Dutrow 1997). A linear least-square fit of $R^{3+} = Al+Fe^{3+}$ plotted versus Mg+Ti yields a regression equation of Mg+Ti = –0.94 * R^{3+} + 8.65 [R=0.990]. Also, correlation of Mg vs. OH+Ti yields OH+Ti = 0.93 * Mg + 1.13 [R=0.944] (Fig. 6c, d). These equations are not consistent with the common Ti substitution mechanism: $Mg^{2+} + Ti^{4+} = 2R^{3+}$ (Henry – Dutrow 1997) and indicate a different mechanism for incorporation of Ti. Its nature is apparent if Ti is plotted versus R^{3+} (Fig. 7), although the nearly linear fit is disturbed by a relatively large error in the OH estimates. This correlation implies the following substitution:

$^{Y}R^{3+} + OH^{1-} = {}^{Y}Ti^{4+} + O^{2-}$ (exchange vector $TiOR^{3+}_{-1}(OH)_{-1}$).

The proposed exchange vector implies coupling of Ti^{4+} incorporation with a decrease of OH and a proportional increase of O. This explains an excellent linear fit of Mg if plotted versus OH+Ti (Fig. 6c). This substitution trends to a potential new Ti-rich tourmaline:

$Na(TiR^{3+}_2)(Mg_2R^{3+}_4)Si_6O_{18}(BO_3)_3((OH)_2O)O$.

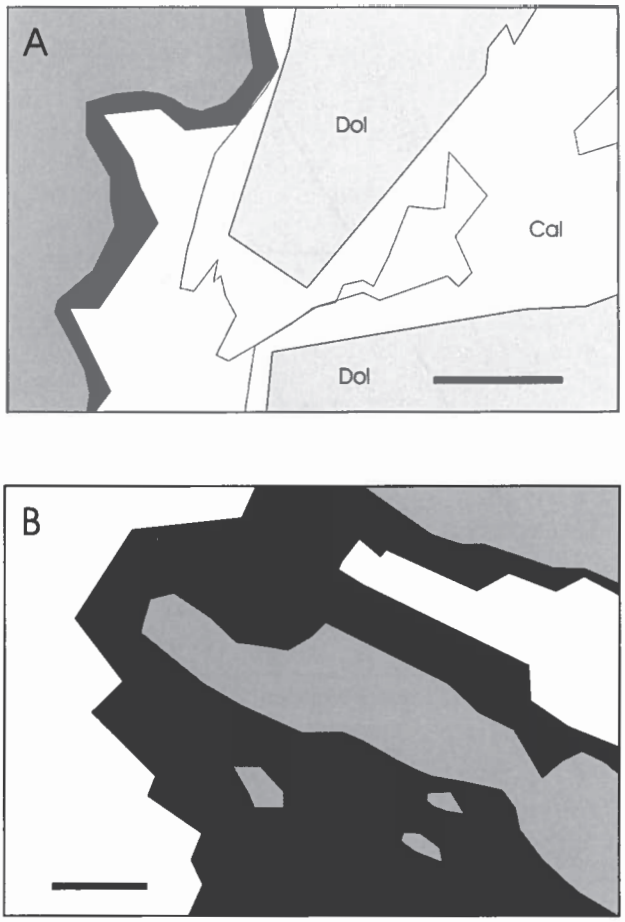

Fig. 3. Line-drawings based on BSE (back-scattered electron) images.
A. Sample 3, large cores of aluminous tourmaline (3a, dark grey) are overgrown with thin povondraite rim (black). Associated minerals are dolomite and calcite.
B. Sample 14, aluminous povondraite (black) replaces older ferrian "oxy-dravite" (14a, grey)
Scale bar represents 100 microns. The cavities are white.

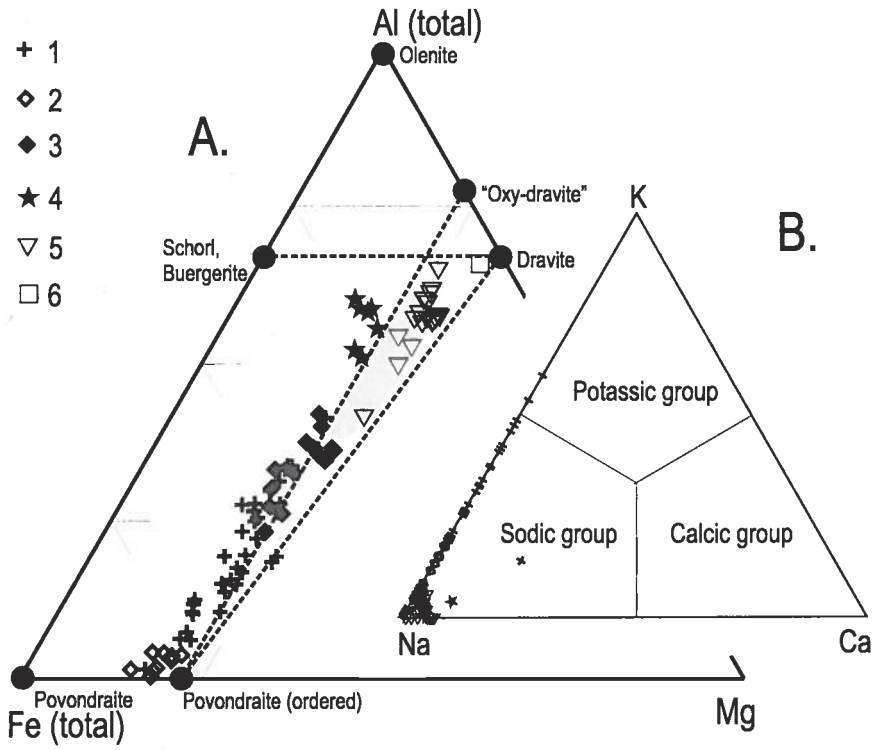

Fig. 4A. Al - $Fe^{3+\,tot}$ – Mg diagram for Alto Chapare tourmalines. The dashed lines represent the schorl (buergerite) – dravite, povondraite – "oxydravite" and povondraite – dravite joins. Shaded area corresponds to tourmaline compositions from Challenger Knox (Henry *et al.* 1999). 1. Povondraite to highly aluminous povondraite, K-rich, mostly Ti-rich; 2. Povondraite, low-Al, low-K, Ti-poor; 3. Intermediate povondraite – "oxy-dravite" – dravite tourmaline, mostly Ti-rich; 4. Ferrian "oxy-dravite"; 5. Ferrian tourmaline of dravite –"oxy-dravite" solid solution; 6. Dravite. For additional characterization of tourmaline groups 1–6 see Table 1 and the Appendix.
Fig. 4B. Na - Ca - K diagram for Alto Chapare tourmalines. *Vacancy* is low, up to 0.11 *apfu*, generally increasing with Ca. *Vacancies* are largely absent if K>0.1 *apfu*. Two compositions correspond to a new potential K-dominant tourmaline species.

Although several tourmaline compositions with Ti>0.5 *apfu* correspond to this potential tourmaline species, more detailed chemical and structural study is necessary to characterize it as a new mineral.

Considering dravite, "oxy-dravite" and "ordered" povondraite as end-member compositions and assuming no Fe^{2+}, all our data should plot among the three, with Mg from 2 to 3 *apfu*. However, many compositions show Mg from ≈ 1.5 to ≈ 2 *apfu* (Fig. 6a–d). There are two possible substitution mechanism. Assuming all iron to be only trivalent this correlation is consistent with exchange vector $R^{3+}O(Mg\ OH)_{-1}$ and results in a hypothetical tourmaline composition $NaFe_3^{3+}(Mg_1\ Fe_5^{3+})\ Si_6O_{18}\ (BO_3)_3\ (OH)_2O_2$ and potentially also a Mg-free povondraite with the end-member formula of Grice *et al.* (1993), $Na\ Fe_3^{3+}\ Fe_6^{3+}\ Si_6O_{18}\ (BO_3)_3O_3OH$. In reality, povondraite (and most probably also additional Alto Chapare ferrian and ferric tourmalines) can contain some minor Fe^{2+} (Grice *et al.* 1993). The amount of Fe^{2+} should be consistent with the increase in OH_{calc}. This implies a shift of data from the least square fit line toward dravite (if Mg in the diagrams is replaced by the sum of R^{2+} = Mg+Fe^{2+}). The quantification of both substitution mechanism is impossible, of course without quantitative analytical data on Fe^{2+}.

The *X-site* is principally occupied by Na. Calcium and *X-site vacancy* attain 0.08 and 0.11 *apfu*, respectively; they increase with increasing Al whereas highly ferrian and ferric tourmalines are mostly Ca-free with no *vacancy* at the *X-site* (Fig. 4b). The values of K/(Na+K) range from 0 to 0.60, and they increase with increasing Fe^{3+} (exchange vector KNa_{-1}). Two compositions with K/(Na+K)>0.5 correspond to a potential new tourmaline species:

$K\ Fe_3^{3+}(Mg_2\ Fe_4^{3+})Si_6O_{18}\ (BO_3)_3\ (OH)_3\ O$,

but no portions of K-dominant tourmaline larger than several tens of microns were observed (Fig. 8, Tab. 2). Similarly, Grice *et al.* (1993) reported 1 composition of K-dominant tourmaline which formed a rim of one of their samples, 10 microns thin.

The composition of Alto Chapare tourmalines

Chemical composition of Alto Chapare tourmalines is highly variable: $Fe^{3+\,tot}$ = 0.31–7.58 *apfu*, Al^{tot} = 0.03–5.81 *apfu*, Mg = 1.32–2.67 *apfu*, Ti = 0.0–0.56 *apfu*, K = 0.0–0.60 *apfu*, OH_{calc} = 1.78–3.52 *apfu*. X-ray powder diffraction data display variations consistent with an extreme compositional range; *unit-cell* dimensions of our povondraite samples are consistent with those described by Grice *et al.* (1993) for type povondraite (Žáček *et al.*, in preparation).

Based on chemical composition, substitution trends and mode of occurrence, our tourmalines were classified into 6 groups (A–F). The ranges of atomic proportions for all tourmaline groups are summarized in Table 1, see also Figs 4–8.

A. Povondraite to highly aluminous povondraite, K-rich, mostly Ti-rich
B. Povondraite Al-poor, K-poor, Ti-poor
C. Intermediate povondraite – "oxy-dravite" – dravite tourmaline, mostly Ti-rich
D. Ferrian "oxy-dravite"
E. Ferrian tourmaline of dravite – "oxy-dravite" solid solution
F. Dravite

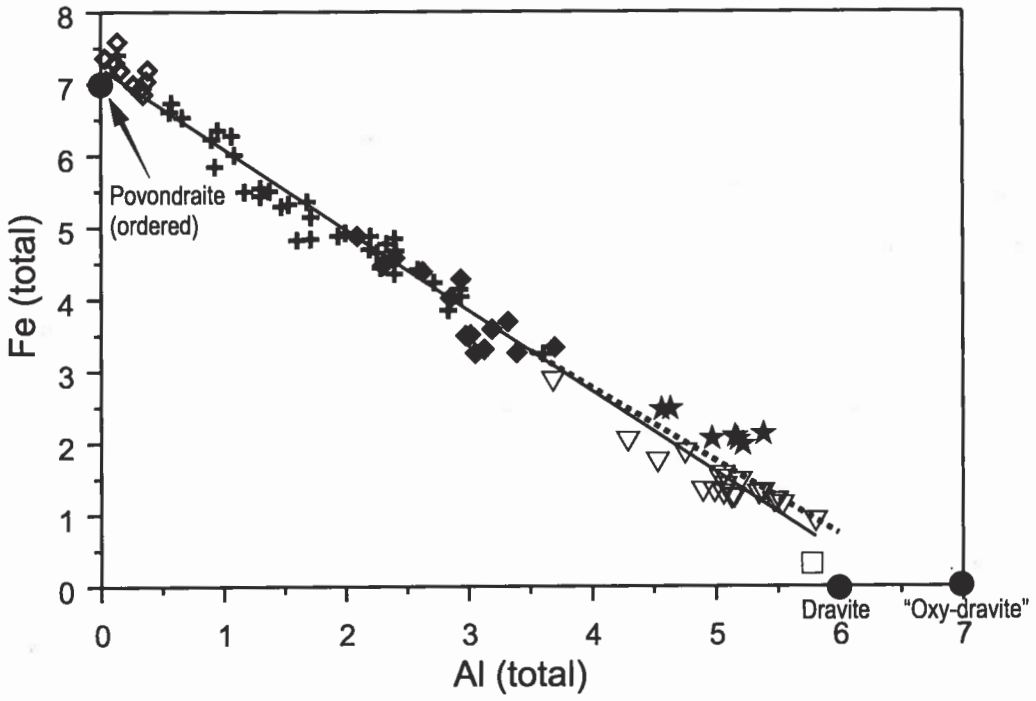

Fig. 5. Relationship of Al^{tot} versus Fe^{tot} for Alto Chapare tourmalines. A linear least-squares fit of the Al (total) plotted versus Fe (total) yielded the regression Fe= –1.12 * Al + 7.21 [R=0.977]. The dashed line represents the regression line of the Challenger Knox cap-rock tourmaline (Henry *et al.* 1999). For explanation of symbols see Fig. 4.

A. Povondraite to highly aluminous povondraite, K-rich, mostly Ti-rich

This group comprises the most abundant Chapare "povondraites" (samples 1, 3, 5, 14, 20, B2, B3). The compositions of type "ferridravite" (Walenta – Dunn 1974) and povondraite (Grice – Ercit 1993) also belong to this group. Tourmaline occurs as crystals, veinlets or massive impregnations. It is associated with crystals of microcline, aegirine and magnesioriebeckite as crystal crusts overgrowing and locally intensively replacing the highly potassic silicate clasts composed predominantly of potassium feldspar with minor phlogopite (see Petrov *et al.* 1997, Žáček *et al.* 1998), The tourmaline crystals are black, short prismatic to stubby up to about 0.5 cm (largely 1–3 mm) in size, and they commonly form complicated mutual intergrowths. The crystals usually have sharply bound cores of ferrian "oxy-dravite" (see group D). The A – group tourmaline corresponds principally to the povondraite – "oxy-dravite" solid solution with widely variable amounts of Fe (from 3.24 to 7.40 *apfu*) and Al (from 0.14 to 3.61 *apfu*), elevated K positively correlated with Fe and strongly variable Ti (mainly from 0.3 to 0.45 *apfu*), see Table 2. Pronounced continuous and locally oscillatory zoning in terms of Al, Fe, K, and Ti is reported by Grice *et al.* (1993) and Žáček *et al.* (1998), but the character of the zoning is highly variable. Two compositions in one sample (#3) with K/(Na+K) >0.5 (0.54 and 0.60) correspond to a potential new K-dominant tourmaline species (Fig. 8, Table 2) but the mean composition of this sample has K/(Na+K) = 0.44.

B. Povondraite low-Al, low K-poor, Ti-poor

Tourmaline of this type is rare and was identified in only two samples (# 15, 22). It occurs in crystal crusts typically associated with hematite crystals. The crystals are small, up to 1 mm long, black and stubby (#15). Sample 22 contains a large core of intermediate povondraite – "oxy-dravite" tourmaline, and povondraite forms only a thin rim. Prismatic shape of the crystals and deep-brown color correspond to the characteristics of the dominant aluminous tourmaline. The povondraite rim #22 and the crystals #15 have extremely low Al amounts (0.03–0.38 *apfu*) and consequently high

Table 1. Compositional ranges of atomic proportions in 6 principal tourmaline groups for tourmalines from Alto Chapare. Atomic contents normalized to the sum of *T*+*Z*+*Y* cations = 15.

group	tourmaline	sample	$Fe^{3+\,tot}$	Al^{tot}	Mg	Ti	K	Ca	OH_{calc}
A.	K-rich (Al) povondraite	B2, B3, 1, 3, 5, 14, 20	3.24–7.40	0.14–3.61	1.49–2.26	0.01–0.56	0.12–0.60*	0	1.78–2.84
B.	Povondraite	15, 22	6.75–7.58	0.03–0.38	1.32–1.84	0.0–0.04	0.13–0.22*	0	2.31–2.74
C.	Intermediate Al-Fe^{3+} tur	B4/2, 3a, 6, 18, 24, 25	3.25–4.88	2.10–3.99	1.64–2.12	0.10–0.50	0.03–0.08	0.0–0.02	2.35–3.00
D.	Fe-"oxydravite"	1a, 6a, 14a, 22a	1.97–2.47	4.56–5.38	1.43–1.92	0.02–0.21	0.0–0.03	0.0–0.08	2.53–2.99
E.	Dravite – ferrian "oxy-tur"	B1, B4/3, 1, 7, 26	0.89–2.84	3.68–5.81	2.20–2.58	0.0–0.34	0.0–0.06	0.0–0.06	3.01–3.52
F.	Dravite	4	0.31	5.78	2.67	0.17	0.01	0	3.49

* K/(Na+K)

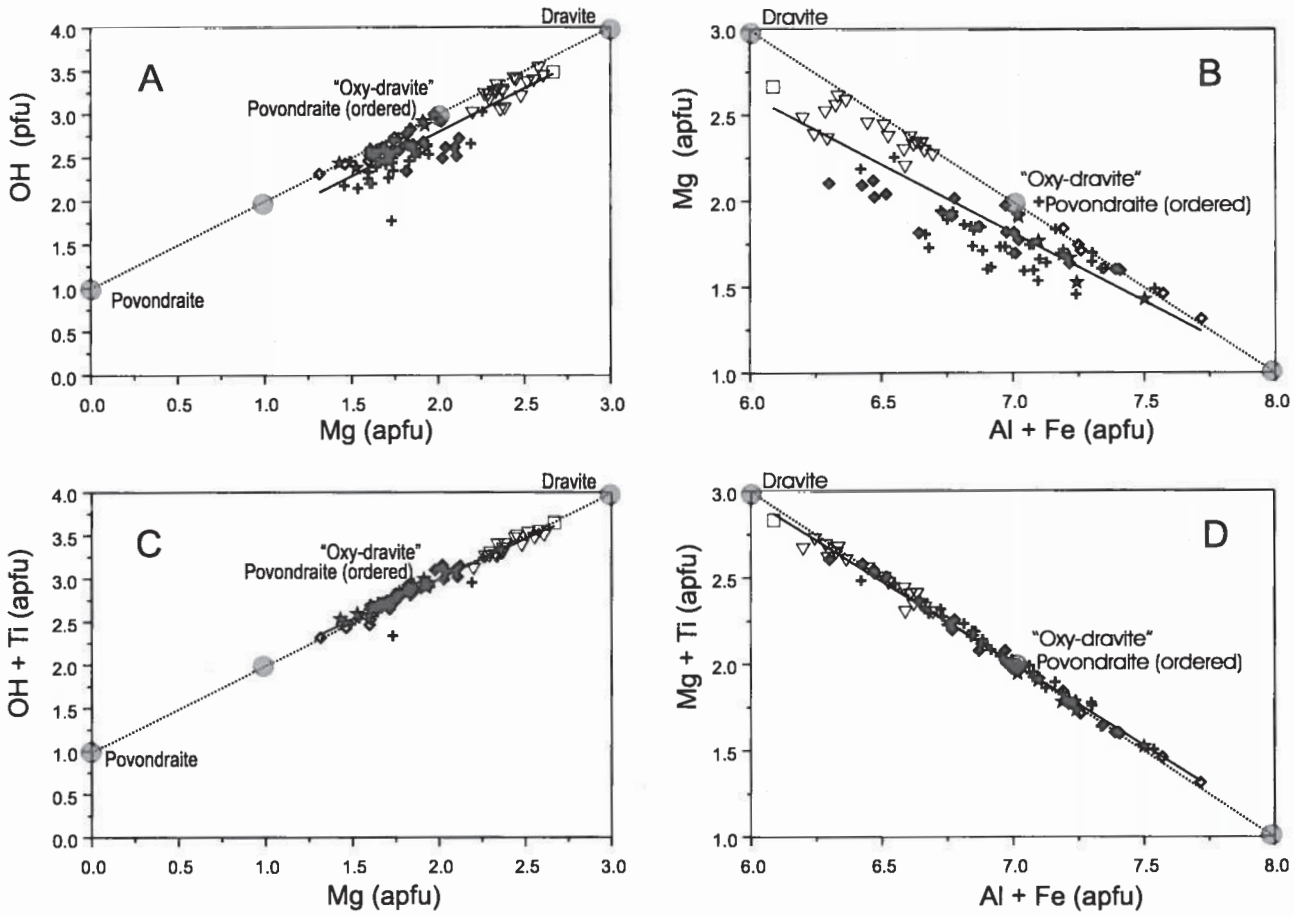

Fig. 6. (**A**) Mg vs. OH calculated, (**B**) Mg vs. R^{3+} (= Al^{tot} + Fe^{tot}), (**C**) Mg vs. OH+Ti, and (**D**) R^{3+} vs. Mg + Ti for Alto Chapare tourmalines (for explanation of symbols see Fig. 4).

The stippled line follows the exchange vector R^{3+} O^{2-} $(Mg\ OH)_{-1}$. Solid lines represent a linear least-squares fit of the data. A linear least-square fit of R^{3+} = Al+Fe^{3+} plotted versus Mg+Ti yields the regression: Mg+Ti = –0.94 * R^{3+} + 8.65 [R=0.990]. Similarly, the Mg vs. OH+Ti yields OH+Ti = 0.93 * Mg + 1.13 [R=0.944].]. These equations are not consistent with common mechanism of Ti substitution: Mg^{2+} + Ti^{4+} = $2R^{3+}$ and they indicate a different mechanism for Ti incorporation: $^{Y}R^{3+}$ + $(OH)^{1-}$ = $^{Y}Ti^{4+}$ + O^{2-} (exchange vector $TiOR^{3+}_{-1}(OH)_{-1}$). From this equation results that Ti amount is equal to the oxygen amount. This explains an excellent linear fit in Fig. 6 C.

Assuming all iron to be trivalent, this correlation is consistent with the exchange vector $R^{3+}O(Mg\ OH)_{-1}$ and results in a hypothetical tourmaline composition $[NaFe_3^{3+}(Mg_1Fe_5^{3+})Si_6O_{18}(BO_3)_3(OH)_2O_2]$ (plotted as non-labeled dot) and potentially also in the Mg-free end-member povondraite formula of Grice *et al.* (1993).

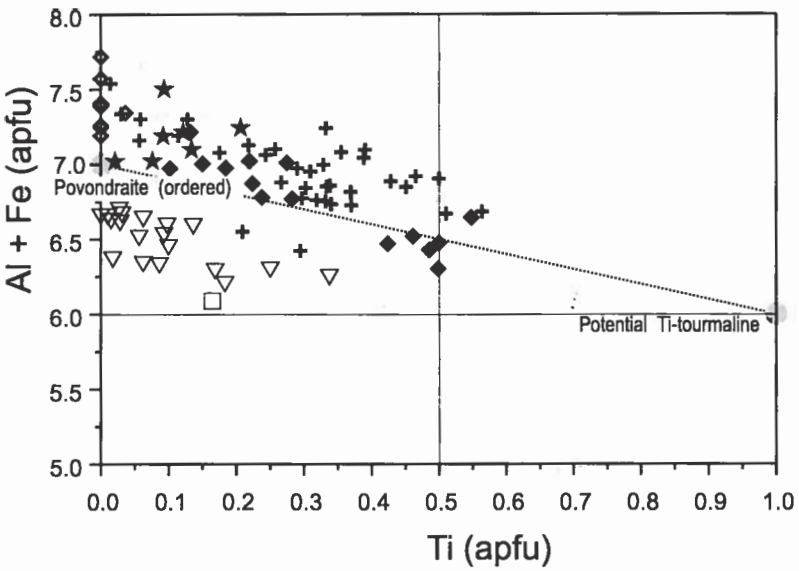

Fig. 7. Ti vs. sum of Al^{tot} + Fe^{tot}. A rough negative linear correlation of Ti and R^{3+} implies the substitution $^{Y}R^{3+}$ + $(OH)^{1-}$ = $^{Y}Ti^{4+}$ + O^{2-} (exchange vector $TiOR^{3+}_{-1}(OH)_{-1}$). This substitution points to a new possible Ti-rich tourmaline: $Na(TiR^{3+}_2)(Mg_2R^{3+}_4)Si_6O_{18}(BO_3)_3((OH)_2O)O$. Several tourmaline compositions with Ti>0.5 *apfu* correspond to this potential tourmaline species. For explanation of symbols see Fig. 4.

Fe (6.75–7.58 *apfu*), relatively low K (0.13–0.22 *apfu*), and Ti largely below the detection limit. Because of the low Al, K, and Ti, this tourmaline is closest to the ideal end-member povondraite (Table 2).

C. Intermediate povondraite – "oxy-dravite" – dravite tourmaline, mostly Ti-rich

Mainly black, crystalline crusts, rarely, black, prismatic crystals, frequently associated with aegirine and magnesioriebeckite. The clasts are commonly bluish, containing K-feldspar, albite and fine magnesioriebeckite but they were not studied in detail. Compositionally, the tourmalines represent K-poor intermediate povondraite – "oxy-dravite" – dravite solid solutions. Their compositions are bizzare with widely varying amounts of Mg (from 1.64 to 2.12 *pfu*), calculated OH (from 2.35 to 3.0 *pfu*) and Ti, (from 0.10 to 0.50 *pfu*), Table 3. The specific name of individual tourmaline compositions would vary, depending on allocation of Al, Fe and Mg (and Ti) into the *Z* and *Y* sites, which is impossible without single-crystal structure refinements.

D. Ferrian "oxy-dravite"

This tourmaline composes only sharply bound cores in some crystals of aluminous povondraite of group A. It was found in # 1, 6, 14, 22 (core compositions are marked as 1a, 6a, 14a, 22a). It represents a K- and Ti-poor ferrian "oxy-dravite" with Fe variable from 2.0 to 2.5 *pfu* (Table 3). Low Mg can indicate a presence of certain amount of Fe^{2+} in a schorl component (see Figs 4a, 6).

E. Ferrian tourmaline of dravite – "oxydravite" solid solution

Tourmaline forms brown needles included as individual crystals in danburite or magnesite, or it forms long-prismatic crystals overgrowing and replacing some silicate

Table 2. Representative tourmaline compositions in groups A and B.

group	A	A	A	A	A	A	B	B	B	B
sample	5	20	1	14	B2	3	15	15	22	22
SiO_2	33.15	32.75	31.09	31.45	30.85	28.66	30.01	30.90	30.49	30.35
TiO_2	2.22	2.24	3.20	2.73	1.82	0.09	0.00	0.00	0.24	0.00
Al_2O_3	16.90	12.58	8.77	7.54	5.99	0.55	0.57	1.15	0.67	[B]0.14
Fe_2O_3[x]	23.76	30.69	33.90	37.64	37.60	47.34	50.68	47.77	48.44	49.41
MnO	0.00	0.00	0.00	0.14	0.00	0.00	0.00	0.00	0.00	0.00
MgO	6.88	6.35	5.62	5.65	6.38	4.81	4.43	6.03	5.47	5.44
CaO	0.00	0.00	0.00	0.00	0.00	0.00	0.00	0.00	0.00	0.00
Na_2O	2.40	2.17	1.89	1.87	1.43	1.06	2.27	2.15	2.24	2.30
K_2O	0.48	0.89	0.98	1.38	1.84	[A]2.39	0.62	0.79	0.59	0.53
Total	85.79	87.67	85.45	88.39	85.91	84.91	88.58	88.79	88.15	88.16
	Atomic contents normalized to the sum of $T + Z + Y$ cations = 15									
Si	6.000	6.004	6.001	5.952	6.004	5.956	5.968	6.005	6.011	6.006
Ti	0.302	0.309	0.465	0.388	0.266	0.014	0.000	0.000	0.036	0.000
Al	3.605	2.718	1.994	1.681	1.373	0.135	0.134	0.263	0.157	0.032
Fe^{3+}	3.236	4.234	4.923	5.361	5.506	7.403	7.584	6.985	7.188	7.357
Mn	0.000	0.000	0.000	0.022	0.000	0.000	0.000	0.000	0.000	0.000
Mg	1.856	1.736	1.617	1.595	1.851	1.491	1.315	1.746	1.609	1.604
total	15.000	15.000	15.000	15.000	15.000	15.000	15.000	15.000	15.000	15.000
Ca	0.000	0.000	0.000	0.000	0.000	0.000	0.000	0.000	0.000	0.000
Na	0.842	0.771	0.707	0.685	0.539	0.427	0.875	0.810	0.858	0.881
K	0.111	0.207	0.241	0.332	0.457	0.635	0.157	0.196	0.147	0.133
X-site	0.953	0.978	0.948	1.018	0.996	1.062	1.031	1.007	1.005	1.014
OH^*_{calc}	2.600	2.445	2.203	2.259	2.585	2.459	2.315	2.735	2.557	2.584

* OH is calculated based on charge balance constraints
[A] composition with highest K_2O concentration
[B] composition with lowest Al_2O_3 concentration
[x] all iron as Fe_2O_3

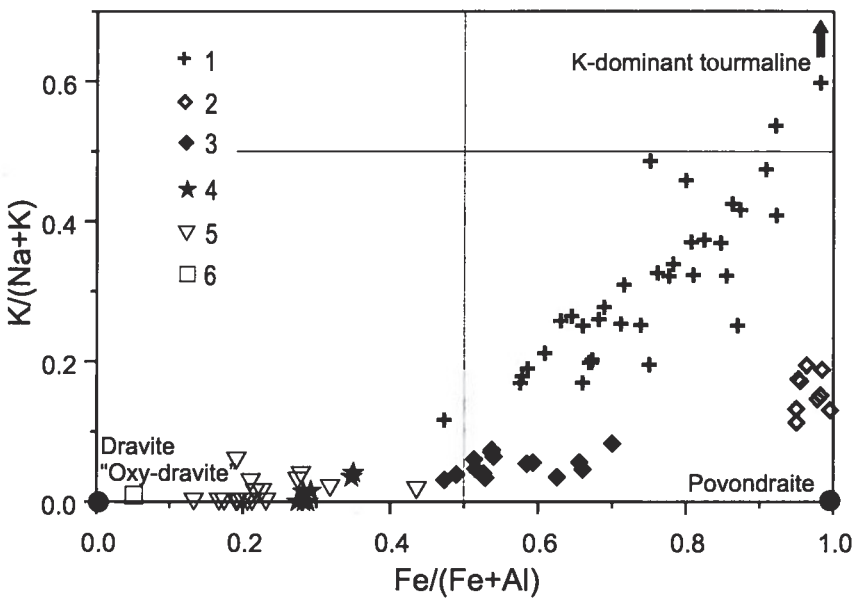

Fig. 8. $Fe^{tot}/(Fe^{tot}+Al)$ vs. K/(Na+K) diagram for Chapare tourmalines. Note that for $Fe^{3+}/(Fe^{3+}+Al) = \approx 1$, the $K_x = \approx 0.5$ (maximum 0.6). 1. Povondraite to highly aluminous povondraite, K-rich, mostly Ti-rich; 2. Povondraite, low-Al, low-K, Ti-poor; 3. Intermediate povondraite – "oxy-dravite" – dravite tourmaline, mostly Ti-rich; 4. Ferrian "oxy-dravite"; 5. Ferrian tourmaline of dravite – "oxy-dravite" solid solution; 6. Dravite.

clasts (26, 7, B1, B4/3). It contains Mg (2.20–2.58 *pfu*) and OH_{calc} (3.01–3.52 *pfu*) in amounts corresponding to the transitional compositions between dravite and "oxy-tourmaline" (ferrian "oxydravite"), (Table 4).

F. Dravite

A unique sample (#4) represents a small clast of sandstone appearance covered by pale brown acicular tourmaline. The clast is composed of fine-grained quartz and minor magnesite and boracite. This tourmaline represents nearly pure dravite containing only 0.31 Fe *apfu*, but 2.67 Mg apfu and 2.5 OH_{calc} *pfu* (Table 4).

Conclusions

No tourmalines have been reported in the literature from evaporite and meta-evaporite deposits which are comparable with Alto Chapare cap rock tourmalines in terms of Al deficiency, as well as high K and Ti (see Deer *et al.* 1997, Henry – Dutrow 1997, Henry *et al.* 1999). Ferrian tourmalines from other (non-evaporite) geological settings have Al>3 *apfu* and in most cases a significant amount of divalent iron (see Henry *et al.* 1999). The ranges of atomic contents for all analyzed Alto Chapare tourmalines are: $Fe^{3+\,tot}$ = 0.31–7.58 *apfu*, Al^{tot} = 0.03–5.81 *apfu*, Mg = 1.32–2.67 *apfu*, Ti = 0.0–0.56 *apfu*. K = 0.0–0.60 *apfu*, OH_{calc} = 1.78–3.52 *apfu*. Alto Chapare tourmalines are principally solid solutions between povondraite, "oxy-dravite" and dravite as end-members (Figs 4a, 5). The most important substitutions are consistent with exchange vectors $FeAl_{-1}$, $R^{3+}O(MgOH)_{-1}$, $TiOR^{3+}{}_{-1}(OH)_{-1}$ and KNa_{-1}.Tourmalines along the povondraite – "oxy-dravite" join (see Fig. 4a) commonly have OH<3 and Mg<2 (Fig. 6a–c), implying that the formula of "ordered" povondraite proposed by Henry *et al.* (1999) need not to be a limiting end-member (see Fig. 6a–d). This problem can be completely solved once the amount of divalent iron could be determined, and structure of the sample refined. The substitution $TiOR^{3+}{}_{-1}(OH)_{-1}$ could lead to a new possible Ti-bearing tourmaline: $Na(TiR^{3+}{}_2)(Mg_2R^{3+}{}_4)Si_6O_{18}(BO_3)_3((OH)_2O)O$ (Fig. 7). Rarely, K/(Na+K) values attain more than 0.5 corresponding to a potential new tourmaline species: $K\,Fe^{3+}{}_3(Mg_2\,Fe^{3+}{}_4)Si_6O_{18}\,(BO_3)_3\,(OH)_3\,O$ (Fig. 8). However, we have not observed segments of K-dominant tourmaline larger than several tens of microns (and neither did Grice *et al.* 1993).

Table 3. Representative tourmaline compositions in groups C and D.

group	C	C	C	C	D	D	D	D
sample	24	25	18	B4/2	1a	14a	6a	22a
SiO_2	32.73	33.14	32.65	32.53	33.64	34.64	34.66	35.08
TiO_2	1.33	0.97	1.98	3.60	1.00	0.16	1.58	0.95
Al_2O_3	11.07	13.76	12.08	13.79	22.08	22.21	25.16	25.70
$Fe_2O_3{}^x$	33.07	31.41	31.62	25.04	18.42	18.75	15.96	15.87
MnO	0.00	0.11	0.00	0.00	0.10	0.00	0.00	0.00
MgO	6.64	6.07	6.18	7.37	6.67	7.41	5.89	6.56
CaO	0.00	0.00	0.08	0.00	0.14	0.41	0.00	0.22
Na_2O	2.54	2.68	2.44	2.68	2.54	2.38	2.70	2.69
K_2O	0.23	0.24	0.14	0.31	0.14	0.16	0.00	0.00
Total	87.63	88.38	87.17	85.32	84.72	86.11	85.94	87.06
	Atomic contents normalized to the sum of $T + Z + Y$ cations = 15							
Si	6.018	5.999	6.017	6.000	5.985	6.035	6.025	5.993
Ti	0.184	0.132	0.274	0.500	0.134	0.021	0.206	0.121
Al	2.400	2.936	2.624	2.997	4.631	4.562	5.155	5.175
Fe^{3+}	4.576	4.278	4.385	3.477	2.466	2.458	2.088	2.040
Mn	0.000	0.017	0.000	0.000	0.015	0.000	0.000	0.000
Mg	1.821	1.637	1.699	2.027	1.770	1.924	1.527	1.670
Ca	0.000	0.000	0.016	0.000	0.027	0.076	0.000	0.040
Na	0.907	0.940	0.874	0.960	0.875	0.806	0.911	0.890
K	0.054	0.056	0.032	0.073	0.032	0.034	0.000	0.000
X-site	0.961	0.996	0.921	1.033	0.933	0.916	0.911	0.930
OH^*_{calc}	2.658	2.527	2.471	2.495	2.706	2.875	2.385	2.585

* OH is calculated based on charge balance constraints

x all iron as Fe_2O_3

Table 4. Representative tourmaline compositions in groups E and F

group	E	E	E	E	E	E	E	F
sample	26	26	7	B4/3	B4/3	B1	B1	4
SiO_2	33.95	35.51	35.00	35.58	35.38	35.97	35.15	36.36
TiO_2	0.70	0.75	2.60	0.79	0.17	0.08	0.49	1.31
Al_2O_3	17.67	23.42	22.29	25.53	29.19	28.13	25.99	29.32
$Fe_2O_3{}^x$	21.36	14.20	13.22	10.81	11.50	8.87	11.27	2.48
MnO	0.00	0.00	0.00	0.00	0.00	0.00	0.00	0.00
MgO	9.01	8.58	9.28	9.75	6.85	9.37	9.25	10.71
CaO	0.15	0.11	0.08	0.06	0.16	0.32	0.00	0.00
Na_2O	2.78	2.72	2.70	2.88	2.86	2.98	2.97	2.88
K_2O	0.07	0.16	0.13	0.00	0.00	0.00	0.06	0.04
Total	85.68	85.46	85.29	85.39	86.11	85.72	85.18	83.11
	Atomic contents normalized to the sum of $T + Z + Y$ cations = 15							
Si	6.006	6.111	6.033	6.001	5.978	6.005	5.962	6.078
Ti	0.093	0.098	0.337	0.100	0.022	0.010	0.063	0.165
Al	3.683	4.752	4.530	5.076	5.813	5.537	5.197	5.776
Fe^{3+}	2.843	1.839	1.715	1.372	1.462	1.115	1.439	0.312
Mn	0.000	0.000	0.000	0.000	0.000	0.000	0.000	0.000
Mg	2.375	2.201	2.385	2.452	1.726	2.333	2.340	2.669
Ca	0.028	0.020	0.015	0.011	0.029	0.056	0.000	0.000
Na	0.952	0.907	0.901	0.942	0.937	0.964	0.976	0.933
K	0.016	0.036	0.028	0.000	0.000	0.000	0.013	0.009
X-site	0.997	0.963	0.943	0.953	0.966	1.020	0.989	0.941
OH^*_{calc}	3.251	3.008	3.057	3.388	2.731	3.241	3.326	3.486

* OH is calculated based on charge balance constraints

x all iron as Fe_2O_3

The povondraite – "oxy-dravite" tourmalines also occur in other meta-evaporite environments (e. g. Popov and Sadykhov 1967, Cabella *et al.* 1987, Henry *et al.* 1999). Some our ferrian "oxy-dravite" – dravite solid solutions (groups D, E) are compositionally very close to the authigenic cap-rock tourmalines from Challenger Knoll, Gulf of Mexico (Henry *et al.* 1999). The course of tourmaline crystallization in Alto Chapare indicates that Fe^{tot} increase and Al decrease for the entire system. Discontinous zoning of tourmaline crystals probably indicates a rapid change (increase?) in P-T conditions. The unique chemistry (highly oxidic, Al-poor K- B- Fe-rich environment) and probably also the changing P-T conditions explain the extreme compositional range of Alto Chapare tourmalines.

Acknowledgments. The authors are oblidged to Dr. I. Vavřín for electron microprobe analyses and to Dr. P. Černý, C. McCracken and Dr. J. B. Selway (The University of Manitoba, Winnipeg, Canada), Dr. S. Vrána (Czech Geological Survey, Praha) and Dr. M. Novák (The Masaryk University, Brno) for critical reviews of the manuscript that substantially improved the interpretations, presentation, and language.

Submitted January 22, 2000

References

Cabella, R. – Cortosogno, L. – Lucchetti, G. (1987): Danburite-bearing mineralizations in metapelites of Permian age (Ligurian, Brianconnais, Maritime Alps, Italy). – N. Jb. Mineral. Mh., 289–294.

Deer, W. A. – Howie. R. A. – Zussman, J. (1997): Rock-forming minerals, Vol. 1B, Disilicates and Ring Silicates, 2nd Ed. The Geol. Soc. London.

Franz, E. D. – Ponce, J. – Wetzenstein, W. (1979): Geochemie und Petrographie der Magnesitlagerstätten des Alto Chapare / Bolivien. – Radex-Rundschau, 4, 1105–1119, Austria.

Grice, J. D. – Ercit, T. S. – Hawthorne, F. C. (1993): Povondraite, a redefinition of the tourmaline ferridravite. – Am. Mineralogist, 78, 433–436.

Hawthorne, F. C. – Henry, D. J. (1999): Classification of the minerals of the tourmaline group. – Eur. J. Mineral., 11, 201–215.

Henry, D. J. – Dutrow, B. L. (1996): Metamorphic tourmaline and its petrologic implications. – Rev. Mineral., 33, 500–555.

Henry, D. J. – Kirkland, B. L. – Kirkland, D. W. (1999): Sector-zoned tourmaline from the cap rock of a salt dome. – Eur. J. Mineral., 11, 263–280.

Petrov, A. (1994): Aktuell: Der Neue Turmalin aus dem tropischen Regenwald Boliviens. – Extra Lapis 6 (Turmalin), 50–53.

Petrov, A. – Hyršl, J. – Žáček, V. (1997): The povondraite occurrence in Alto Chapare, Cochabamba, Bolivia. – Abstr., Tourmaline 1977 – Inter. Symp. on Tourmaline, June 20–25th, Nové Město na Moravě, 68–69.

Popov, V. S. – Sadykhov, T. S. (1962): Authigenic tourmaline from the Khodzha-Mumyn salt deposit. – Dokl. Akad. Nauk. SSSR, 145, 140–141.

Walenta, K. – Dunn, P. J. (1977): Ferridravite, a new mineral of the tourmaline group from Bolivia. – Am. Mineralogist, 64, 945–948.

Žáček, V. – Petrov, A. – Hyršl, J. (1998): Chemistry and origin of povondraite-bearing rocks from Alto Chapare, Cochabamba, Bolivia. – Jour. Czech Geol. Soc., 43/1–2, 59–67. Praha.

Turmalíny řady povondrait – (oxy)dravit ze sádrovcového klobouku metaevaporitu v Alto Chapare, provincie Cochabamba, Bolívie

Na typové lokalitě povondraitu v Alto Chapare, v provincii Kočabamba v Bolívii se vyskytují železité, Al-deficitní turmalíny, které téměř zcela pokrývají možné pole složení mezi povondraitem – „oxy-dravitem" a dravitem. Tyto turmalíny se vyskytují jako součást krystalických kůr, které obrůstají klasty silikátových hornin původně uzavřených v metaevaporitu nebo jako inkluze v evaporitových minerálech. Krystaly turmalínu jsou morfologicky velmi proměnlivé od jehlicovitých přes sloupcovité až po izometrické, přičemž habitus odráží jejich chemické složení. Některé krystaly turmalínu jsou diskontinuálně zonální s jádry tvořenými Al-bohatším turmalínem než okraje. Chemicky jsou to sodné turmalíny s velmi nízkými obsahy Ca a s nízkou *vakancí* na pozici *X*. Železem bohaté a hliníkem chudé členy mají obvykle zvýšené koncentrace draslíku (až 0.6 *pfu*) a tvoří přechod k možného novému koncovému členu „K-povondraitu". Všechny turmalíny jsou hořečnaté (Mg = 1.32–2.67 *apfu*) a vykazují extrémní variabilitu v chemickém složení. Hlavní substituce Fe^{3+} (0.31–7.58 *apfu*) za Al (0.03–5.81 *apfu*) odpovídá vektoru $Fe(Al)_{-1}$. Železem bohaté členy tvoří přechod mezi povondraitem $[NaFe_3^{3+}(Mg_2Fe_4^{3+})Si_6O_{18}(BO_3)_3(OH)_3O]$ a hypotetickým členem $[NaFe_3^{3+}(Mg_1Fe_5^{3+})Si_6O_{18}(BO_3)_3((OH)_2O)O]$. V souladu s tímto substitučním mechanismem, množství OH (vypočtené ze vzorce) kolísající v rozmezí 1.78–3.52 *pfu* pozitivně koreluje s obsahem Mg a negativně koreluje se sumou trojmocných kationtů R^{3+} (= Al + Fe^{3+}). Substituce Ti^{4+} je spjata s poklesem OH a růstem O. Velmi variabilní titan (0.0–0.56 *apfu*) negativně koreluje se sumou trojmocných kationtů. Celkově, suma trojmocných kationtů velmi dobře negativně koreluje se sumou Mg+Ti (R = 0.99). Výše uvedená fakta jsou v souladu se substitučními vektory $R^{3+}O(MgOH)_{-1}$ a $TiOR^{3+}{}_{-1}(OH)_{-1}$. Substituce titanu vede k formulaci chemického vzorce možného Ti-turmalínu: $Na(TiR^{3+}{}_2)(Mg_2R^{3+}{}_4)Si_6O_{18}(BO_3)_3((OH)_2O)O$.

Pevné roztoky mezi povondraitem a „oxy-dravitem" byly popsány i z jiných meta-evaporitových turmalínů, ale zdaleka nedosahují tak velkého chemického rozpětí jako na typové lokalitě povondraitu v Bolívii.

Appendix – a review of the samples studied:

B–1 Acicular brown tourmaline on apple-green massive fine-grained rock; tourmaline also forms metacrysts within the clast.

B–2 Fine-grained black tourmaline crystal crust on grey-brown clast composed of dominant K-feldspar and minor phlogopite. Tourmaline also forms veinlets in the clast.

B–3 Massive, speckled clast composed mainly of K-feldspar and black tourmaline with accessory phlogopite, hematite and sagenitic rutile.

B–4 Gray, fine-grained rock composed of K-feldspar, phlogopite and minor pyrite; tourmaline occurs as rare microscopic accessory in the matrix. Tourmaline porphyroblasts (dravitic B4/3) enclose small cores of titanian ferrian "oxy-tourmaline" (B4/2).

#1 Large angular grey-green clast (10x8x7 cm, Fig. 2) showing several episodes of fracturing (different faces of this clast show tourmaline crystal crusts of varying crystal size and type), followed by fracturing without tourmaline growth. Coarser crust is composed of black stubby well-developed tourmaline crystals 0.2–2 mm long, the other one is coherent, finer-grained, with the crystal size up to 1 mm. Tourmaline also replaces the interior of the clast. Larger crystals have a core of aluminous tourmaline (1a).

#3 Dark grey–bluish clast composed of potassium feldspar?, magnesioriebeckite and minor pyrite. Crystalline crust is sharply bound, composed of well developed, 1–2 mm long, prismatic, black, brownish translucent tourmaline crystals associated with microcline, dolomite, calcite and pyrite. BSE image indicate two sharply bound tourmaline generations, older aluminous tourmaline (3a) and younger povondraite (3).

#4 Light brown translucent tourmaline needles 2–4 mm long grown on colorless medium-grained crystalline material composed of predominant quartz and minor magnesite and boracite.

#5 Black fine-crystalline tourmaline crust about 1 cm thick replaces a light rock composed mainly of potassium feldspar; the crystals are poorly developed and associated with 1–3 mm long pyrite crystals.

#6 Small (1 cm) clast composed of predominant short prismatic black tourmaline and younger grass-green prismatic aegirine. On fractures and in BSE, overgrowth of a black tourmaline rim (6) on an older (pale brown) aluminous tourmaline (6a) is visible. Dipyramidal honey-brown TiO_2 crystals (probably anatase, up to 0.5 mm long) and colorless microcline are minor components.

#7 Brown danburite crystal clouded by tiny acicular tourmaline inclusions.

#14 Loose tourmaline clast – radiating tourmaline aggregate with fibers up to 12 mm long and multiple crystal terminations, minor mineral is microcline. BSE image indicates an older more aluminous tourmaline (14a) and ferric rim (14).

#15 Sharply bound crystalline crust composed of ankerite, hematite and pyrite crystals with minor tourmaline. Tourmaline forms isolated, well-developed, stubby, flattened crystals 1–2 mm long. Sequence: pyrite – hematite – tourmaline – ankerite. The youngest mineral is pale blue magnesioriebeckitic asbestos. The composition of the fine-grained sandstone-like clast was not studied.

#18 Rare type of clast, reddish, composed of quartz, albite and potassium feldspar, aegirine with minor magnesioriebeckite and microscopic tourmaline.

#20 Light clast composed of prevailing K-feldspar is nearly completely overgrown by crust composed of abundant 1–2 mm long tourmaline crystals. They are black, stubby and display complicated mutual intergrowths. Accessory pyrite and microcline crystals occur.

#22 Black, sharply bounded 1 mm thick crust composed of small prismatic, deep-brown translucent tourmaline crystals, accompanied by platy hematite; magnesioriebeckite is younger. BSE images show a large core of aluminous tourmaline (22a) overgrown by a thin rim of povondraite (22).

#24 Black, microcrystalline tourmaline crust, locally brown–green translucent, with poorly developed tourmaline crystals, microcline and magnesioriebeckite; the clast is bluish–grey colored by magnesioriebeckite.

#25 Massive, fine-grained black tourmaline crust up to 1 cm thick replaces a bluish clast rich in potassium feldspar and magnesioriebeckite. Short prismatic, brown, translucent tourmaline crystals (up to 1 mm long), younger sky-blue prismatic magnesioriebeckite and grass-green aegirine crystals occur in cavities.

#26 Coarse-granular dolomite encloses numerous acicular tiny tourmaline crystals, besides rare pyrite. The clast is locally covered with bluish magnesioriebeckitic asbestos.